Compact, Low Profile, Common Aperture Polarization, and Pattern Diversity Antennas

Jungsuek Oh, *Member, IEEE*, and Kamal Sarabandi, *Fellow, IEEE*

***Abstract*—This paper presents compact and low profile two-port antennas that can provide polarization or pattern diversity schemes from a common aperture. The proposed antennas make use of a novel small microstrip antenna topology with an open area at its waist. The two sections of the small-size microstrip antenna are connected through a magnetic coupling mechanism facilitated by two vertical metallic strips connecting the top plates to the ground plane. This allows for placement of another small antenna element within the same aperture having either polarization or pattern that is orthogonal to the microstrip antenna with low envelope correlation. Topologies of polarization and pattern-diversity antennas are optimized for size reduction and minimum envelope correlation. Although the proposed diversity antenna consists of two antenna elements with different polarizations or radiation patterns, they just occupy about 30% of the area of a conventional microstrip antenna over the same substrate. It is shown that the envelope correlation between radiation patterns of the two antenna elements is lower than −30 dB over the 10-dB return loss bandwidth of the proposed antenna.**

***Index Terms*—Antennas diversity, microstrip antennas, multiple-input–multiple-output (MIMO) systems.**

I. Introduction

THE requirement for the next generation of mobile communication systems calls for high speed and high quality data transmission of the mobile terminals. This makes multiple-input–multiple-output (MIMO) technology attractive for its excellent performance improvement in channel capacity without occupying additional spectrum and radiating power [1]. MIMO systems have emerged as a very interesting strategy to increase the capacity of wireless systems in rich scattering environments [2], [3]. Traditionally, MIMO systems employ several transmit and receive antennas at each end of the radio link, and this can achieve higher data rates (capacity), if different signal paths between them are statistically uncorrelated. In the existing MIMO systems, antenna diversity is a well-known technique to enhance the performance of wireless communication systems by reducing the multipath fading and cochannel interference [4]–[6]. The idea is based on gathering multiple uncorrelated copies of the signals and effectively combining them for enhanced reception.

There are five different types of diversity techniques that are commonly used for enhanced signal reception: 1) spatial; 2) temporal; 3) polarization; 4) frequency; and 5) pattern. Of these, only the spatial, polarization and pattern diversity schemes make for practical implementation in WLAN antenna systems. The spatial diversity approach relies on placement of multiple antennas at least half a wavelength apart over the platform to be effective. Since the desired long separation among the diversity antennas require large platforms, polarization and pattern diversity are most appropriate for small wireless devices. Polarization diversity uses different orthogonally-polarized antennas to capture signals with different multipath history. The pattern diversity scheme takes advantage of the incoherence of the rays with sufficiently different angle of arrivals. Antennas with almost angularly orthogonal radiation patterns collect different rays and thus can provide multiple outputs that are statistically uncorrelated. This can be done easily with antennas having relatively narrow beams that are pointed at different directions. However, large volume that antennas in such diversity systems occupy remains a critical problem in implementing small wireless platforms. Previous efforts mainly concentrated on reducing the size of individual antennas for such applications [7], [8]. However, compact colocated diversity antennas have not been well studied. The current approach to achieve antenna diversity is based on placing two or more individual compact antennas in optimized positions that provide low envelope cross-correlation coefficients. This approach is good but the overall volume that the antennas occupy increases directly with their number and eventually the volume becomes too large for compact wireless devices.

With low-cost fabrication and low-profile structure, microstrip antennas are widely used in mobile communication systems [9], [26]. However, due to their relatively large lateral dimension and limited configurations for providing polarization and pattern diversity, these antennas have not been extensively used for the diversity systems. Of course conventional antennas can easily provide dual polarization operation, but such antennas cannot easily be miniaturized [10]–[12]. For example in [10], the size of such antennas is reduced by inserting a number of slits at the perimeter of a square patch. However, since the two orthogonal modes share one patch plate, it is difficult to control the two modes independently. This limits how far the antenna can be miniaturized. Recently, another way for achieving compact diversity microstrip antenna was proposed [13], [14]. In [13], using a circular patch and hybrid feed network, two degenerate modes, TM_{11} and TM_{01}, are

Manuscript received February 05, 2013; revised August 22, 2013; accepted October 02, 2013. Date of publication November 20, 2013; date of current version January 30, 2014. This work was supported in part by the U.S. Army Research Laboratory under contract W911NF and prepared through collaborative participation in the Microelectronics Center of Micro Autonomous Systems and Technology (MAST) Collaborative Technology Alliance (CTA) and the NSF under contract ECCS 1101868.

The authors are with the Radiation Laboratory, Department of Electrical Engineering and Computer Science, University of Michigan at Ann Arbor, Ann Arbor, MI 48109-2122 USA (e-mail: jungsuek@umich.edu; saraband@eecs.umich.edu).

Color versions of one or more of the figures in this paper are available online at http://ieeexplore.ieee.org.

Digital Object Identifier 10.1109/TAP.2013.2291901

excited at an overlapped frequency range. While TM_{11} mode radiates in broadside direction, TM_{01} mode radiation pattern resembles that of a dipole, hence leading to pattern diversity from a common aperture.

Recent advanced RF technologies enable a significant size reduction in RF front-end for wireless communication systems operating at low frequencies such as low UHF-band. This makes it possible to employ the fundamental advantages of low-frequency systems over commercial higher-frequency systems such as 2.4 GHz ISM band in terms of multipath fading effects and path loss. In [24], a new 450 MHz radiation pattern diversity system is presented. The paper shows that incorporating small antennas, radiation pattern diversity offers a unique opportunity to achieve compact diversity antenna systems compared to approaches that utilize spatial diversity. In this paper, we present a novel small-size 450 MHz microstrip antenna that can achieve a significant size reduction while providing polarization and pattern diversity around 450 MHz. Taking advantage of the geometry and field distributions, compact size and low envelope correlation are achieved for both types of diversity antennas. In Section II, design and performance characteristics of the proposed microstrip antenna are presented. In Section III, novel compact polarization and pattern diversity antennas employing the proposed microstrip antenna element are proposed and their envelope correlation and diversity gain are discussed.

II. Novel Small-Size Microstrip Antenna Topology for Compact Common Aperture Design

This section presents a novel microstrip antenna whose geometry enables not only size reduction, but also polarization or pattern diversity with low envelope correlation between two common aperture antenna elements. The basic idea is to split the conventional microstrip antenna into two segments, producing an open area between them. The two segments are then connected though magnetic coupling using shorting strips at the adjacent ends, as shown in Fig. 1(a). Fig. 2 shows voltage and current distributions on the conventional $\lambda_g/2$ microstrip antenna with x-polarized radiation on an infinite ground plane where λ_g is the guided wavelength. In the middle of the antenna, the voltage is at minimum $(= \mathrm{zero})$ and the current is at maximum. This suggests that placement of the shorting strip in the middle of the patch where the zero voltage and maximum current conditions are satisfied does not affect the desired operation of the microstrip antenna. In the proposed antenna, an open area in the middle is introduced. However, it is conjectured that the two adjacent shorting strips through a strong magnetic coupling can provide a continuous current distribution over the two halves of the split patch antenna, which is essential to achieve the desired broadside radiation pattern. The second antenna segment shown on the right side of Fig. 1(a) can be considered as a magnetically coupled parasitic element that allows for maintaining the bandwidth of the original antenna. It should be noted that unlike $\lambda_g/2$ microstrip antenna a shorted $\lambda_g/4$ microstrip antenna cannot provide the ideal broadside radiation pattern due to the omnidirectional and vertically polarized radiation produced from vertical shorting strips. Fig. 1(b) shows the small-size bow-tie version of the proposed microstrip antenna, which will be used to design the proposed diversity antennas in the next sections.

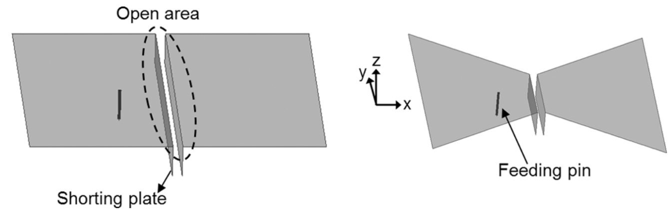

Fig. 1. (a) Proposed microstrip antenna with an open area in its middle and (b) bow-tie version of the proposed microstrip antenna over an infinite ground plane.

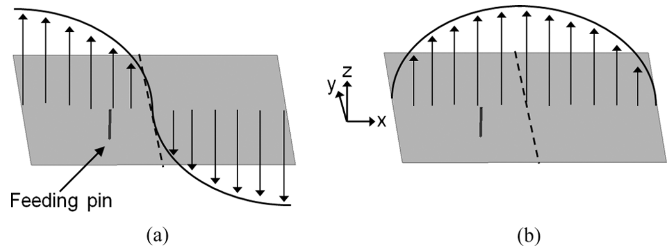

Fig. 2. Distributions of (a) voltage and (b) current on the $\lambda_g/2$ microstrip antenna with x-polarized radiation over an infinite ground plane.

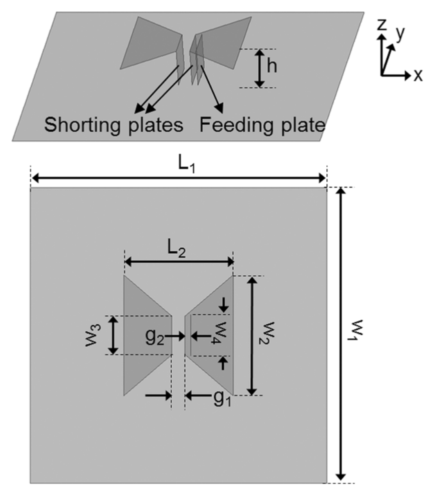

Fig. 3. Geometry and design parameters of the small-size bow-tie version of the proposed microstrip antenna with an open area at its waist.

Fig. 3 shows the geometry and design parameters of the proposed bow-tie microstrip antenna on a finite ground plane. Impedance matching to a 50 ohm feed line is obtained by controlling g_2 (the distance between the feeding strip and the shorting strip on the right side), similar to conventional $\lambda_g/2$ microstrip antennas. The values of design parameters are given by $L_1 = 500$ mm, $L_2 = 182$ mm $(= 0.27\lambda_g)$, $w_1 = 500$ mm, $w_2 = 204$ mm $(= 0.3\lambda_g)$, $w_3 = 65$ mm, $w_4 = 70$ mm, $g_1 = 20$ mm, $g_2 = 10$ mm and $h = 60$ mm $(= 0.09\lambda_g)$. Fig. 4 shows simulated S_{11} of the proposed antenna. Two resonant frequencies are observed and Fig. 5 shows the current distributions at the two resonant frequencies. At the first resonant frequency, horizontal currents on one trapezoidal top plate are in the opposite direction to the horizontal currents on the other top plate, leading to the cancellation of the radiated fields from the top plates. On the other hand, at the second resonant frequency, the horizontal currents on both top plates have the same

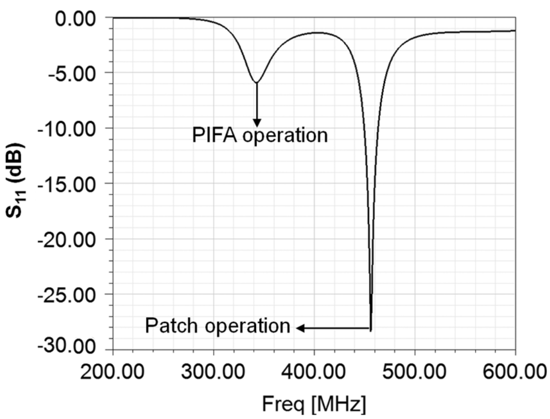

Fig. 4. Simulated S_{11} of the proposed bow-tie microstrip antenna shown in Fig. 3.

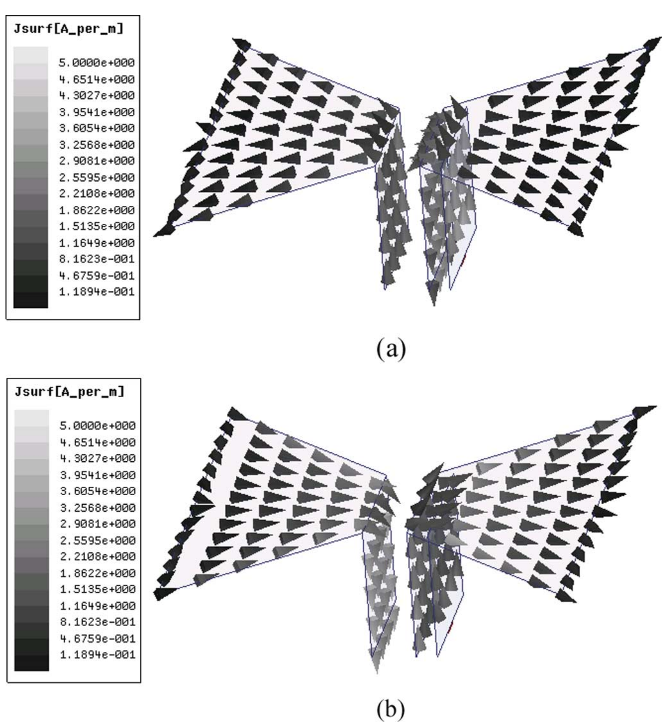

Fig. 5. Current distributions of the proposed antenna in Fig. 3 at (a) 342 MHz (PIFA mode) and (b) 456 MHz (patch mode).

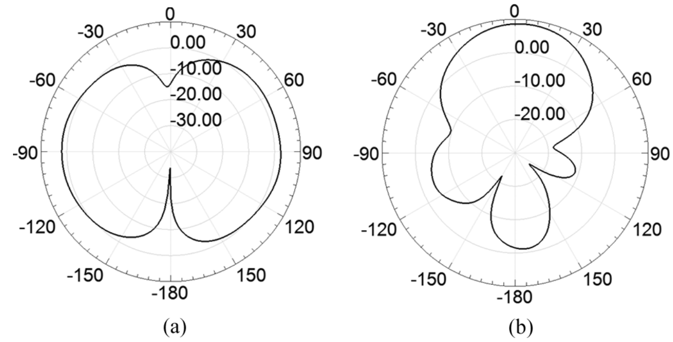

Fig. 6. Simulated radiation patterns (gain) of the proposed bow-tie microstrip antenna on E-plane (xz-plane) at two resonant frequencies, corresponding to (a) PIFA mode and (b) patch mode. Antenna geometry is shown in Fig. 4.

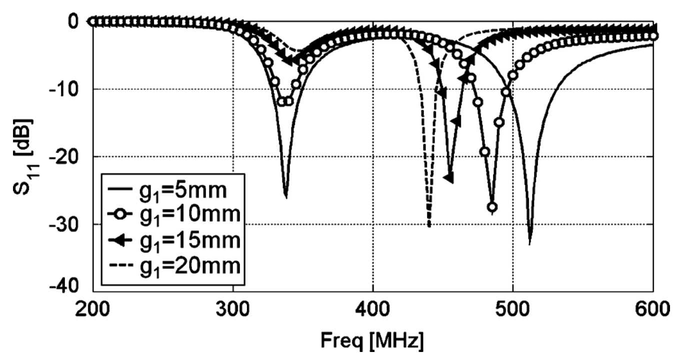

Fig. 7. Simulated S_{11} of the proposed bow-tie microstrip antenna versus g_1.

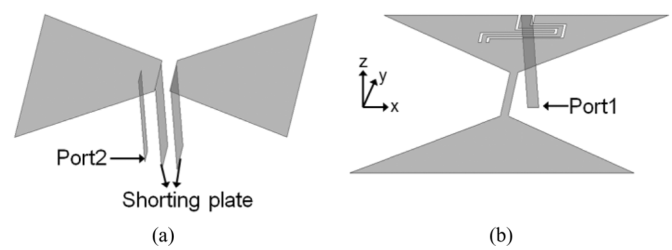

Fig. 8. (a) Proposed bow-tie microstrip antenna with x-pol and (b) conventional bow-tie microstrip antenna with y-pol.

direction. As a result, the antenna has omnidirectional radiation pattern in the H-plane at the first resonant frequency (denoted by 'PIFA mode'), and it has broadside radiation pattern at the second resonant frequency (patch mode), as shown in Fig. 6.

In this paper, design parameters are optimized for the patch-mode operation at the second resonant frequency. Fig. 7 shows simulated S_{11} as a function of g_1 while other parameters are kept constant. It is shown that as g_1 increases, the second resonant frequency decreases due to the increase in the overall antenna volume. However, the antenna bandwidth decreases with increasing g_1. This is because of a significant drop in the magnetic coupling between two shorting plates related to the stored magnetic energy responsible for the antenna bandwidth.

III. Compact Common Aperture Diversity Antennas

A. Design of Polarization Diversity Antenna

The aforementioned open area in the proposed bow-tie microstrip antenna allows for insertion of the second antenna with a different polarization into the same aperture. The second antenna must also be miniaturized to fit the available aperture between the bowtie patch. Fig. 8 shows the two antenna elements: 1. Proposed bow-tie microstrip antenna with polarization along x-axis, 2. Conventional bowtie microstrip antenna with polarization along y-axis. As mentioned before, the metallic trace in the middle of the conventional bowtie microstrip antenna shown in Fig. 8(b) can be placed in the open area of the two-section microstrip antenna shown in Fig. 8(a). Fig. 9 shows the geometry and design parameters of the proposed polarization diversity antenna. To excite the desired patch operation, the position of the feeding strip should be near the center of the microstrip antenna as shown in Fig. 8(a). However, placing a feeding strip for the second antenna near its waist becomes problematic as it will be

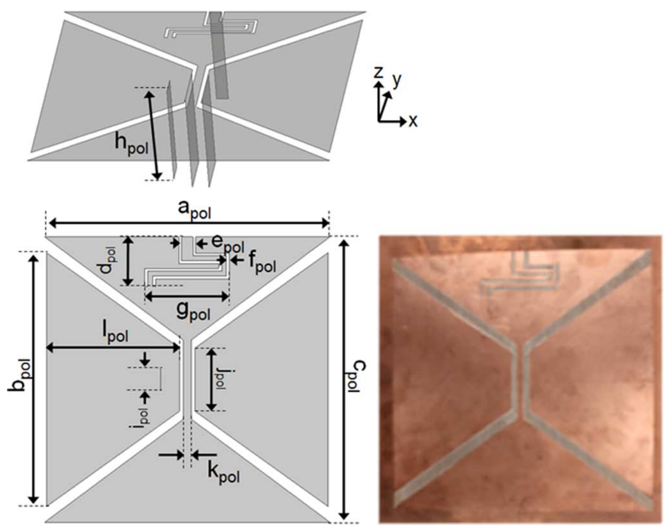

Fig. 9. Geometry and design parameters of the proposed polarization diversity antenna.

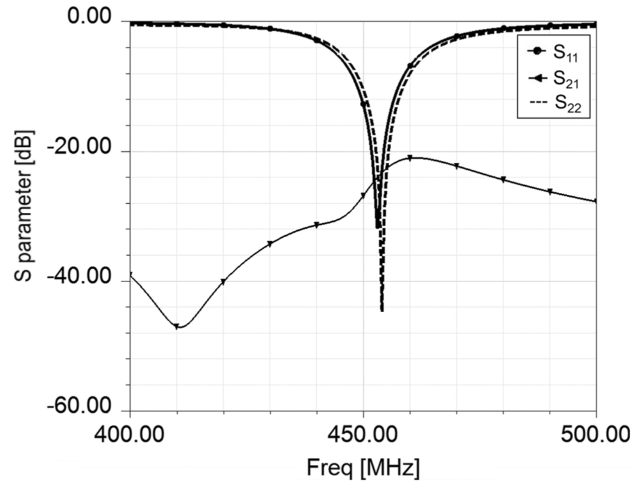

Fig. 10. Simulated S_{11}, S_{21} and S_{22} of the proposed polarization diversity antenna.

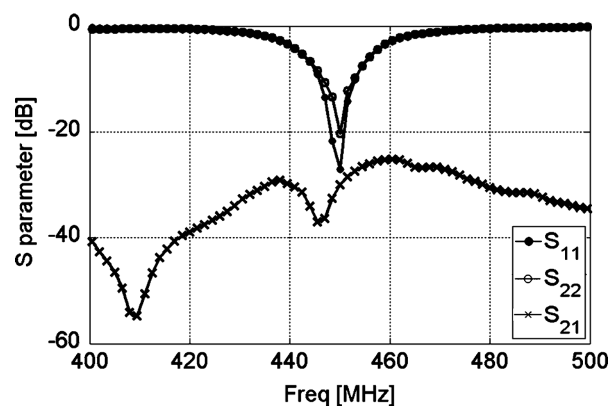

Fig. 11. Measured S_{11}, S_{21} and S_{22} of the proposed polarization diversity antenna.

too close to the feed of the other antenna. Close proximity of the feeds creates significant magnetic mutual coupling and results in poor polarization isolation. For this reason, the feeding strip position is moved back to the open end using a meandered coplanar waveguide (CPW) line as shown in Fig. 8(b). This minimizes the undesired coupling between the two feeding strips connected to "port1" and "port2," respectively. The length of the meandered CPW transmission line is chosen to be $\lambda/4$ to act as an impedance transformer for impedance matching between the antenna and the feed [25]. The width of the center line and the gap between the center line and the ground are chosen for the desired characteristic impedance value of the transmission line.

Design parameters and their values for the proposed antenna designed in the air without using any dielectric substrate are shown in Table I. Fig. 10 shows simulated S_{11}, S_{21} and S_{22} of the proposed polarization diversity antenna. Resonant frequencies of the two antenna elements are merged to 454 MHz at which the isolation between two ports (S_{21}) is -23.3 dB. In Fig. 11, the measured S-parameters show good agreement with the simulated results. The area of the proposed diversity antenna is just 29.7% of the area of a conventional microstrip antenna with the dimension of $\lambda_g/2 \times \lambda_g/2$ operating at the same frequency. Another advantage of this antenna configuration is its ability to operate at slightly different two resonant frequencies corresponding to the two antenna elements. As mentioned in Section I, the two ports of most conventional dual polarized small-size microstrip antennas share a single top plate which limits the level of size reduction. However, in the proposed design, each antenna element has its individual top plate. Since the two antenna elements are physically separated, the change in the geometry of an antenna element has a minimal impact on the resonant frequency of the other antenna element. Fig. 12 shows simulated S_{11}, S_{21} and S_{22} of the proposed polarization diversity antenna by varying l_{pol}. Fig. 12(a) and (b), respectively, show variations in S-parameters when l_{pol} is increased or decreased by 5 mm from its nominal value. As expected, while the resonant frequency corresponding to the antenna element connected to "port2" (S_{22}) is slightly shifted, the other resonant frequency related to "port1" (S_{11}) doesn't change. This characteristic of the proposed topology can be utilized to design compact tunable diversity antennas.

The diversity gain is a function of the antenna efficiency, envelope-correlation (ρ_e), and the relative signal strength levels between the two received signals [12]. In order to achieve a reduction in signal fading and thus a higher level of diversity gain, the following two conditions must be satisfied [4]:

$$\rho_e < 0.5 \quad \text{and} \quad P_1 \approx P_2 \tag{1}$$

where P_i is the average signal strength received at each branch of the antenna and ρ_e is envelope-correlation. The envelope correlation can be obtained using radiation patterns or S-parameters which are described in detail in [6] and [15], respectively. In this paper, the envelope correlation is calculated from the S-parameters by using

$$\rho_e = \frac{|S_{11}^* S_{12} + S_{21}^* S_{22}|^2}{(1 - (|S_{11}|^2 + |S_{21}|^2))(1 - (|S_{22}|^2 + |S_{12}|^2))}. \tag{2}$$

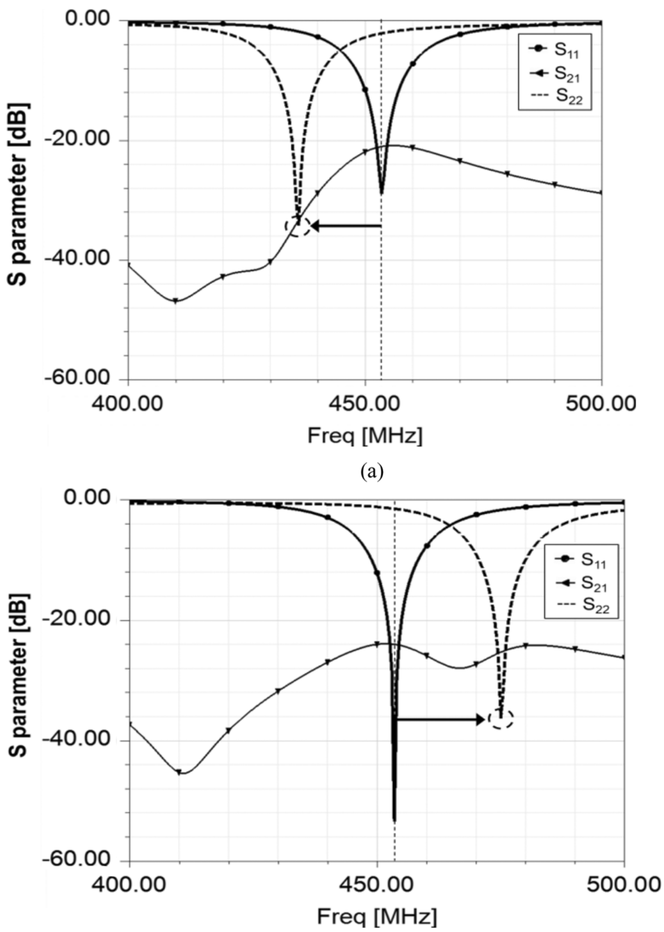

(a)

(b)

Fig. 12. Simulated S_{11}, S_{21} and S_{22} of the proposed polarization diversity antenna with 5 mm (a) increased or (b) decreased l_{pol}.

TABLE I
DESIGN PARAMETERS AND THEIR VALUES OF THE PROPOSED POLARIZATION DIVERSITY ANTENNA. ALL PHYSICAL DIMENSIONS ARE IN MM

a_{pol}	b_{pol}	c_{pol}	d_{pol}	e_{pol}	f_{pol}
180 (=0.27λ_g)	160	180 (=0.27λ_g)	63.3	10.6	1.8
g_{pol}	h_{pol}	i_{pol}	j_{pol}	k_{pol}	l_{pol}
53.2	60	14	40	5	83.8

The formula assumes uniformly distributed radio channel and lossless antennas [16]. Based on [17], as the measured total efficiency of the proposed antennas is high over the operating impedance bandwidth, the effect of the losses on the diversity performance is assumed to be small. Effective diversity gain (EDG) can be obtained by using a selection combining criteria with maximum apparent diversity gain at 1% outage rate [18]. The EDG is calculated by multiplying the diversity gain with the radiation efficiency of the antenna element

$$\mathrm{EDG} = e_{\mathrm{rad}} \cdot 10.48\sqrt{1-|\rho|^2} \qquad (3)$$

where the relation between the complex cross-correlation (ρ) and envelope correlation (ρ_e) is$|\rho|^2 \approx \rho_e$.

Fig. 13 shows the simulated radiation efficiency over the fractional 3-dB return loss bandwidth of the proposed bowtie microstrip antenna. As the operating frequency increases, the radiation efficiency of the antenna fed at Port 1 decreases slightly due to higher ohmic loss and impedance mismatch in the CPW transmission line that occupies a part of the antenna structure. Fig. 14 shows the envelope correlation and EDG obtained from measured S parameters and (2). It is found that the measured envelope correlation (ρ_e) between the two antenna elements is lower than -30 dB over the 10-dB return loss bandwidth of the proposed microstrip antenna. Fig. 15 shows radiation patterns on E-planes of the two bowtie microstrip antennas at 450 MHz. For both antennas, the desired broadside radiation patterns and the co- to cross-pol ratio of more than 10 dB are observed.

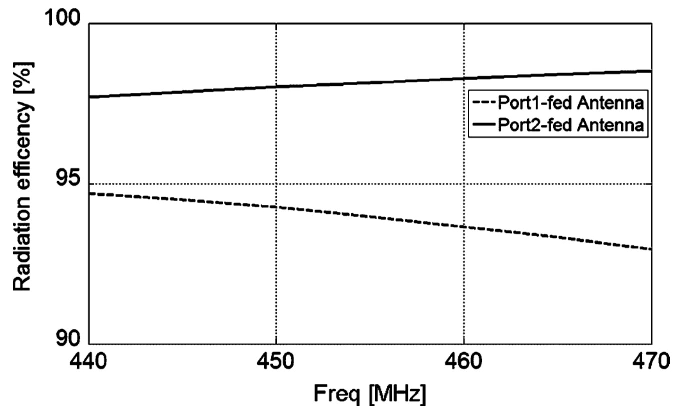

Fig. 13. Simulated radiation efficiency of two antenna elements in the proposed polarization diversity antenna.

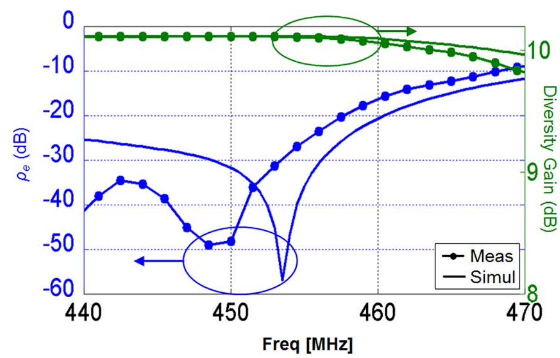

Fig. 14. Envelope correlation (ρ_e) between the two common aperture antenna elements in the proposed polarization diversity antenna and its diversity gain.

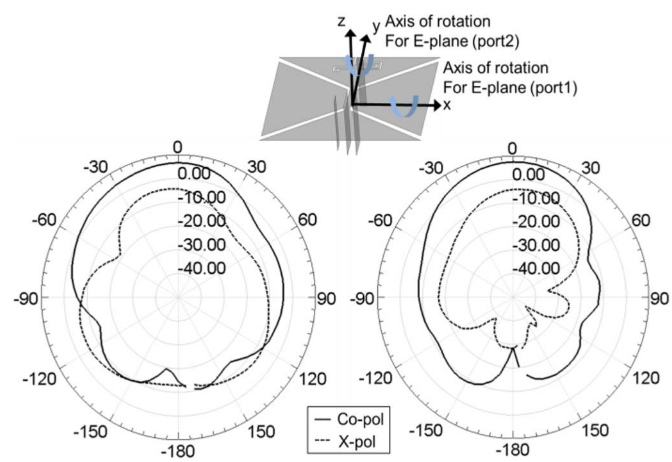

(a)

(b)

Fig. 15. Measured radiation patterns (gain) on E-planes of two bow-tie microstrip antennas: (a) Port1: ON and Port2: OFF (50 Ω terminated) and (b) Port1: OFF (50 Ω terminated) and Port2: ON.

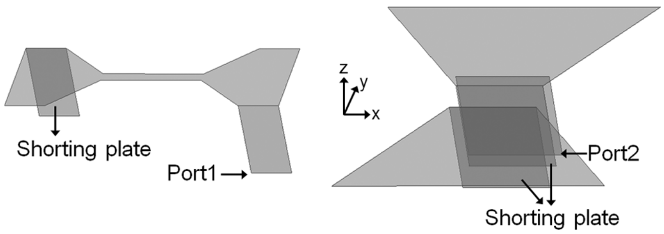

(a) (b)

Fig. 16. (a) Folded monopole antenna with omnidirectional radiation pattern and (b) proposed bowtie microstrip antenna with broadside radiation pattern.

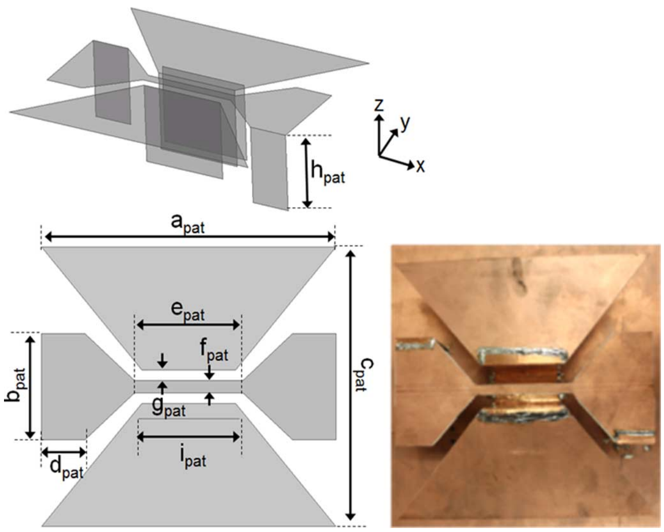

Fig. 17. Geometry and design parameters of the proposed pattern diversity antenna.

B. Design of Pattern Diversity Antenna

This section presents a novel compact pattern diversity antenna utilizing the proposed bowtie microstrip antenna. The proposed pattern diversity antenna consists of the small-size bowtie microstrip antenna and a folded monopole antenna placed in the aforementioned open area between the two segments of the small-size bowtie microstrip antenna. The broadside radiation pattern of the bowtie microstrip antenna and horizontally omnidirectional radiation pattern of the folded monopole antenna achieve the desired radiation pattern diversity. Fig. 16 shows the folded monopole antenna and the small-size bowtie microstrip antenna. The folded monopole antenna is based on the shorted $\lambda_g/2$ transmission line resonator. For the selection of the positions of shorting and feeding strips in the folded monopole antenna, particular attention must be paid to minimize the undesired radiation from the horizontal currents on the top strip [19], [27]. Impedance matching to a 50 Ω feed line can be obtained by tuning e_{pat} and f_{pat} since a short segment (e_{pat}) can work as an impedance transformer [20]. Fig. 17 shows the geometry and design parameters of the proposed pattern diversity antenna. The values of the design parameters are shown in Table II.

At the resonant frequency of the $\lambda_g/2$ folded monopole antenna, voltage is maximum and current is minimum in the middle of the antenna, and thus input impedance at the node in the middle toward the proposed bowtie microstrip antenna is ideally infinite. This property can provide a desired low envelope correlation for the proposed pattern diversity antenna.

TABLE II
DESIGN PARAMETERS AND THEIR VALUES OF THE PROPOSED PATTERN DIVERSITY ANTENNA. ALL PHYSICAL DIMENSIONS ARE IN MM

a_{pat}	b_{pat}	c_{pat}	d_{pat}	e_{pat}	f_{pat}
200 (=0.3λ_g)	70	180 (=0.27λ_g)	30	75	8
g_{pat}	h_{pat}	i_{pat}			
7	60 (=0.09λ_g)	70			

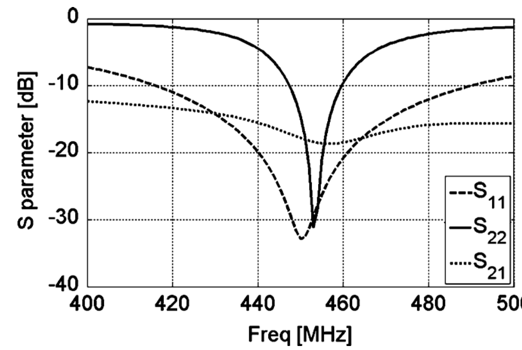

Fig. 18. Simulated S_{11}, S_{21} and S_{22} of the proposed pattern diversity antenna.

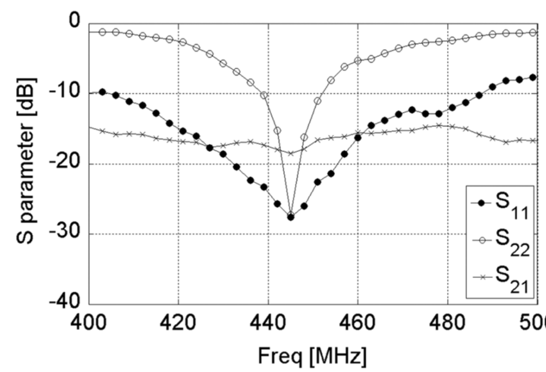

Fig. 19. The measured S_{11}, S_{21} and S_{22} of the proposed pattern diversity antenna.

However, it should be noted that the parasitic in-plane coupling between the top plates of two antenna elements causes a small increase in the envelope correlation. Fig. 18 shows the simulated S_{11}, S_{21} and S_{22} of the proposed polarization diversity antenna. Resonant frequencies of the two antenna elements are tuned to 455 MHz at which the isolation between two ports (S_{21}) is -18.6 dB. In Fig. 19, the measured S-parameters show good agreement with the simulated results. The area of the proposed diversity antenna is just 32% of the area of the conventional microstrip antenna with the dimension of $\lambda_g/2 \times \lambda_g/2$. While the folded monopole antenna is relatively broadband, the microstrip antenna is inherently a narrowband antenna [20]. However, it is well known that the narrow bandwidth of the microstrip antenna can be enhanced by using broadband feeding structures such as the L-shaped probe feeding technique [21], proximity coupling by etching an H-shaped slot [22], and the capacitive feed technique [23]. For broadband diversity applications, the same approaches can be also utilized for the proposed bowtie microstrip antenna.

Fig. 20 shows the simulated radiation efficiency over the 3-dB return loss bandwidth of the proposed bowtie microstrip antenna. Fig. 21 shows envelope correlation and EDG obtained from measured S parameters and (2). It is found that the measured envelope correlation (ρ_e) between radiation patterns of

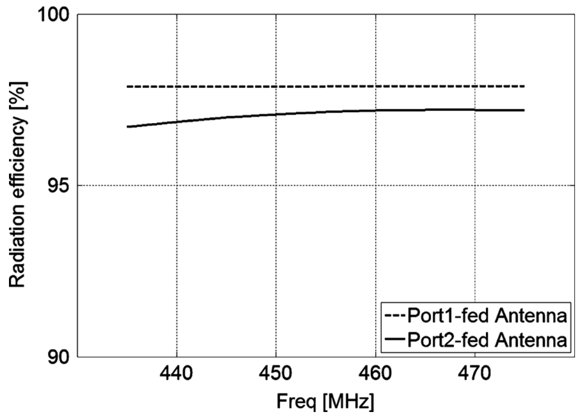

Fig. 20. Simulated radiation efficiency of two antenna elements in the proposed pattern diversity antenna.

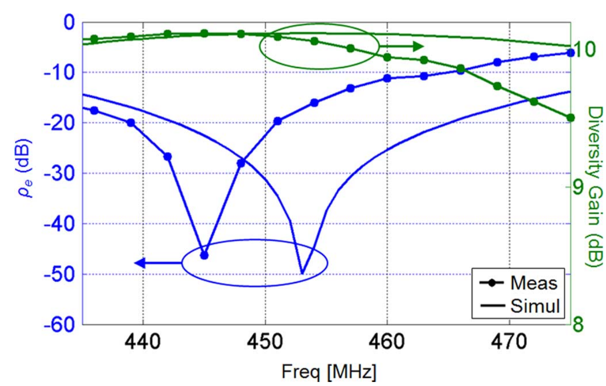

Fig. 21. Envelope correlation (ρ_e) between radiation patterns of two antenna elements in the proposed pattern diversity antenna and its diversity gain.

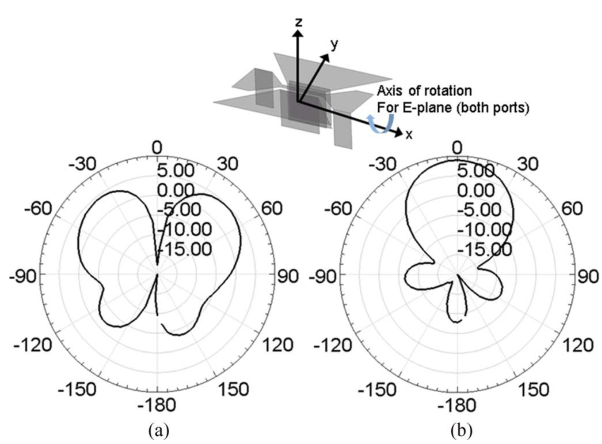

Fig. 22. Measured radiation patterns (gain) on E-planes of the folded monopole antenna and proposed bow-tie microstrip antenna: (a) Port1: ON and Port2: OFF (50 Ω terminated) and (b) Port1: OFF (50 Ω terminated) and Port2: ON.

the two antenna elements is lower than -30 dB over the 10-dB return loss bandwidth of the proposed microstrip antenna. Fig. 22 shows the measured radiation patterns on E-planes of the folded monopole antenna and proposed bowtie microstrip antenna. For the respective antenna element, the desired omnidirectional or broadside radiation pattern is observed, respectively. For all polarization and pattern diversity antennas discussed in this paper, the ground plane with the dimensions of 500 mm by 500 mm is used. It should be noted that if the ground plane gets smaller than half wavelength ($\approx$330 mm at 450 MHz), impedance matching between antennas and feeds needs to be redesigned and center frequency increases.

IV. Conclusion

Compact low profile common aperture polarization and pattern diversity antennas employing a novel microstrip antenna topology are presented. The proposed microstrip antenna consists of two inverted L elements that stands back to back, producing an open area between the two elements. Since the two elements are magnetically coupled through the shorting strips connected to each element, placing another planar antenna element in the open area enables the design of compact diversity antennas with low envelope correlation. It is shown that the area of the proposed diversity antennas is just about 30% of the area of the conventional microstrip antenna with the dimension of $\lambda_g/2 \times \lambda_g/2$. For both types of the proposed diversity antennas, the envelope correlations lower than -30 dB are achieved over the 10-dB return loss bandwidth of the proposed small-size microstrip antenna. The size of the proposed antennas can be further miniaturized by manipulating the degree of tapering in the bow-tie shape and employing high-index (ε_r) material substrate at the expense of bandwidth and gain drop.

References

[1] G. J. Foschini and M. J. Gans, "On limits of wireless communications in a fading environment when using multiple antennas," *Wireless Pers. Commun.*, vol. 6, pp. 311–335, 1998.

[2] T. Svantesson, "Correlation and channel capacity of MIMO systems employing multimode antennas," *IEEE Trans. Veh. Technol.*, vol. 51, no. 6, pp. 1304–1312, Nov. 2002.

[3] P. S. Kildal and K. Rosengren, "Correlation and capacity of MIMO systems and mutual coupling, radiation efficiency, and diversity gain of their antennas: Simulations and measurements in a reverberation chamber," *IEEE Commun. Mag.*, vol. 42, no. 12, pp. 104–112, Dec. 2004.

[4] R. G. Vaughan and J. B. Andersen, "Antenna diversity in mobile communications," *IEEE Trans. Veh. Technol.*, vol. 36, no. 4, pp. 147–172, Nov. 1987.

[5] P. Mattheijssen, M. Herben, G. Dolmans, and L. Leyten, "Antenna pattern diversity versus space diversity for use at handhelds," *IEEE Trans. Veh. Technol.*, vol. 53, no. 4, pp. 1035–1042, Jul. 2004.

[6] M. A. Jensen and Y. Rahmat-Samii, "Performance analysis of antennas for hand-held transceivers using FDTD," *IEEE Trans. Antennas Propag.*, vol. 42, no. 8, pp. 1106–1113, Aug. 1994.

[7] X. Wang, Z. Feng, and K. Luk, "Pattern and polarization diversity antenna with high isolation for portable wireless devices," *IEEE Antennas Wireless Propag. Lett.*, vol. 8, pp. 209–211.

[8] F. Thudor and A. Louzir, "An extremely compact pattern diversity antenna for WLAN," in *Proc. IEEE AP-S Int. Symp.*, Jun. 2002, vol. 4, pp. 60–63.

[9] I. J. Bahl and P. Bhartia*, Microstrip Antennas*. Norwood, MA, USA: Artech House, 1980.

[10] D. T. Notis, P. C. Liakou, and D. P. Chrissoulidis, "Dual polarized microstrip patch antenna, reduced in size by use of peripheral slits," in *Proc. Eur. Conf. Wireless Technol.*, Amsterdam, The Netherlands, 2004, pp. 125–128.

[11] K. Gosalia and G. Lazz, "Reduced size, dual polarized microstrip patch antenna for wireless communications," *IEEE Trans. Antennas Propag.*, vol. 51, no. 9, pp. 2182–2186, Sep. 2003.

[12] S. Hu, J. Pang, and J. Qiu, "A compact polarization diversity MIMO microstrip patch antenna array with dual slant polarizations," presented at the IEEE Int. Symp. Antennas Prop., 2009.

[13] K. Wei, Z. Zhang, W. Chen, and Z. Feng, "A novel hybrid-fed patch antenna with pattern diversity," *IEEE Antennas Wireless Propag. Lett.*, vol. 9, pp. 562–565, 2010.

[14] Z. J. Zhang *et al.*, "Three designs of polarization diversity antenna for WLAN application," presented at the Int. Workshop Antenna Technol. (iWAT'11), Piscataway, NJ, USA, Mar. 2011, IEEE, 2011.

[15] S. Blanch, J. Romeu, and I. Cotbella, "Exact representation of antenna system diversity performance from input parameter description," *Electron. Lett.*, vol. 39, no. 9, pp. 705–707, May 2003.

[16] M. Sonkki, E. Antonino-Daviu, M. Ferrando-Bataller, and E. T. Salonen, "Planar wideband polarization diversity antenna for mobile terminals," *IEEE Antennas Wireless Propag. Lett.*, vol. 10, pp. 939–942, 2011.

[17] P. Hallbjörner, "The significance of radiation efficiencies when using S-parameters to calculate the received signal correlation from two antennas," *IEEE Antennas Wireless Propag. Lett.*, vol. 4, pp. 97–99, 2005.

[18] M. Schwartz, W. R. Bennett, and S. Stein, *Communication Systems and Techniques*. New York, NY, USA: IEEE Press, 1996.

[19] J. Oh and K. Sarabandi, "Low profile, miniaturized, inductively coupled capacitively loaded monopole antenna," *IEEE Trans. Antennas Propag.*, vol. 60, no. 3, pp. 1206–1213, Mar. 2012.

[20] J. Oh and K. Sarabandi, "Low profile vertically polarized omnidirectional wideband antenna with capacitively coupled parasitic elements," *IEEE Trans. Antennas Propag.*, 2013, to be published.

[21] H. Wong, K. L. Lau, and K. M. Luk, "Design of dual-polarized L-probe patch antenna arrays with high isolation," *IEEE Trans. Antennas Propag.*, vol. 52, no. 1, pp. 45–52, Jan. 2004.

[22] S. Gao and A. Sambell, "Dual-polarized broad-band patch antennas fed by proximity coupling," *IEEE Trans. Antennas Propag.*, vol. 53, no. 1, pp. 526–531, Jan. 2005.

[23] K. L. Wong and T. W. Chiou, "Broad-band dual-polarized patch antennas fed by capacitively coupled feed and slot-coupled feed," *IEEE Trans. Antennas Propag.*, vol. 50, no. 3, pp. 346–351, Mar. 2002.

[24] F. T. Dagefu, J. Oh, J. Choi, and K. Sarabandi, "Measurements and physics-based analysis of co-located antenna pattern diversity system," *IEEE Trans. Antennas Propag.*, vol. 61, no. 11, pp. 5724–5734, Nov. 2013.

[25] D. M. Pozar, *Microwave Engineering*, 3rd ed. New York, NY, USA: Wiley, 2004.

[26] J. Oh and K. Sarabandi, "A topology-based miniaturization of circularly polarized patch antennas," *IEEE Trans. Antennas Propag.*, vol. 61, no. 3, pp. 1422–1426, Mar. 2013.

[27] J. Oh, J. Choi, F. T. Dagefu, and K. Sarabandi, "Extremely small two-element monopole antenna for HF band applications," *IEEE Trans. Antennas Propag.*, vol. 61, no. 6, pp. 2991–2999, Jun. 2013.

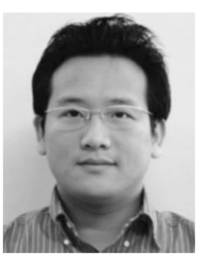

Jungsuek Oh (S'08) received the B.S. and M.S. degrees from Seoul National University, Korea, in 2002 and 2007, respectively, and the Ph.D. degree from the University of Michigan at Ann Arbor, Ann Arbor, MI, USA, in 2012.

From 2007 to 2008, he was with Korea Telecom as a Hardware Research Engineer working on the development of flexible RF devices. In 2012, he was a Postdoctoral Research Fellow with the Radiation Laboratory, the University of Michigan. He is currently a Staff RF Engineer with Samsung Research America-Dallas. His research areas include mmW beam focusing/shaping techniques, antenna miniaturization for integrated systems and radio propagation modeling for indoor scenarios. He has published more than 30 technical journal and conference papers.

Dr. Oh is the recipient of the 2011 Rackham Predoctoral Fellowship Award at the University of Michigan. He has served a Technical Reviewer for the IEEE ANTENNA AND WIRELESS PROPAGATION LETTERS and the IEEE TRANSACTIONS ON ANTENNAS AND PROPAGATION.

Kamal Sarabandi (S'87–M'90–SM'92–F'00) received the B.S. degree in electrical engineering from the Sharif University of Technology, Tehran, Iran, in 1980, the M.S. degree in electrical engineering in 1986, and the M.S. degree in mathematics and the Ph.D. degree in electrical engineering from the University of Michigan at Ann Arbor, Ann Arbor, MI, USA, in 1989.

He is currently the Director of the Radiation Laboratory and the Rufus S. Teesdale Professor of Engineering in the Department of Electrical Engineering and Computer Science, The University of Michigan at Ann Arbor. His research areas of interest include microwave and millimeter-wave radar remote sensing, meta-materials, electromagnetic wave propagation, and antenna miniaturization. He possesses 25 years of experience with wave propagation in random media, communication channel modeling, microwave sensors, and radar systems and leads a large research group including two research scientists, 16 Ph.D. students. He has graduated 42 Ph.D. and supervised numerous postdoctoral students. He has served as the Principal Investigator on many projects sponsored by the National Aeronautics and Space Administration (NASA), Jet Propulsion Laboratory (JPL), Army Research Office (ARO), Office of Naval Research (ONR), Army Research Laboratory (ARL), National Science Foundation (NSF), Defense Advanced Research Projects Agency (DARPA), and a large number of industries. Currently he is leading the Center for Microelectronics and Sensors funded by the Army Research Laboratory under the Micro-Autonomous Systems and Technology (MAST) Collaborative Technology Alliance (CTA) program. He has published many book chapters and more than 226 papers in refereed journals on miniaturized and on-chip antennas, meta-materials, electromagnetic scattering, wireless channel modeling, random media modeling, microwave measurement techniques, radar calibration, inverse scattering problems, and microwave sensors. He has also had more than 530 papers and invited presentations in many national and international conferences and symposia on similar subjects.

Dr. Sarabandi served as a member of NASA Advisory Council appointed by the NASA Administrator for two consecutive terms from 2006–2010. He is serving as a Vice President of the IEEE Geoscience and Remote Sensing Society (GRSS) and is a member of the Editorial Board of the IEEE PROCEEDINGS. He was an Associate Editor of the IEEE TRANSACTIONS ON ANTENNAS AND PROPAGATION and the IEEE SENSORS JOURNAL. He is a Member of Commissions F and D of URSI. He was the recipient of the Henry Russel Award from the Regent of The University of Michigan. In 1999 he received a GAAC Distinguished Lecturer Award from the German Federal Ministry for Education, Science, and Technology. He was also a recipient of the 1996 EECS Department Teaching Excellence Award and a 2004 College of Engineering Research Excellence Award. In 2005 he received the IEEE GRSS Distinguished Achievement Award and the University of Michigan Faculty Recognition Award. He also received the best paper Award at the 2006 Army Science Conference. In 2008 he was awarded a Humboldt Research Award from The Alexander von Humboldt Foundation of Germany and received the Best Paper Award at the IEEE Geoscience and Remote Sensing Symposium. He was also awarded the 2010 Distinguished Faculty Achievement Award from the University of Michigan. The IEEE Board of Directors announced him as the recipient of the 2011 IEEE Judith A. Resnik medal. He was recognized by the IEEE GRSS with its 2013 Education Award. In the past several years, joint papers presented by his students at a number of international symposia (IEEEAPS'95, '97, '00, '01, '03, '05, '06, '07; IEEEIGARSS '99,'02, '07; '11 IEEE IMS'01, USNC URSI'04, '05,' 06, '10, '11 AMTA'06, URSI GA 2008) have received best paper awards.